A Steerable Landing Gear for Vehicles with Main Gear Skids

UPSHUR T. JOYNER*
NASA Langley Research Center, Hampton, Va.

The lifting body spacecraft being developed by NASA and the Air Force will have a landing "footprint" area hundreds of miles long and wide. This gives the opportunity to maneuver to a landing on many conventional airport runways. A ground steering capability will be required. Previous vehicles of this general type, for example, X-15 and Dyna Soar, used main gear skids because of advantages in weight and simplicity, but no directionally stable steering system was available to provide directional control on the ground. A suitable steering system, based on a new concept to be described, is now under development. The system consists of a freely castoring corotating wheel nose gear with an axle that can be tilted right or left under pilot control, and skids on the main gear. A prototype gear used in research has developed a maximum usable steer force, orside force, of about 500 lb, with an applied vertical load of 2000 lb. This amount of steering force is shown to be sufficient to prevent the HL-10 vehicle from leaving the side of a 150-ft-wide runway following touchdown on centerline with a lateral drift rate of 25 fps.

Nomenclature

C_1 = constant of proportionality between tire load and tire vertical deflection ($\delta_0 = C_1W$)
c.g. = center of gravity
D_m,D_n = ground drag forces, main gear and nose gear
F_D = aerodynamic drag of vehicle
F_s = steering force at nose gear
F_x = braking or driving force of each tire in a corotating pair
F_Y = aerodynamic side force acting on vehicle
h = height of c.g. of vehicle above the ground
I = moment of inertia of the vehicle around Z axis
K_x = tire fore-and-aft spring constant
M_m,M_n = moments of main gear and nose gear ground plane forces around the vertical axis through c.g.
M_s = steering moment applied around steer axis
M_Z = aerodynamic yawing moment around Z axis
$M\dot{\psi}$ = aerodynamic moment around Z axis due to yawing velocity
M_t = moment applied to tilt the axle to obtain differential tire loading
N = cornering power of a tire
p,q = distances along the centerline of the vehicle from the c.g. to the main gear and to the nose gear, respectively
q_g = geometric castor of the nose gear
q_p = pneumatic castor of the nose gear tire
r_e = effective rolling radius
r = undeflected radius of tire
s = spacing between tire centerlines on a corotating wheel nose gear
t = effective castor, or trail of the nose gear ($q_g + q_p$)
V = vehicle forward speed
W = vehicle weight
W_m,W_n = weights on the main gear and nose gear
W_l,W_r = weights on the left and right tires of a corotating wheel nose gear
x = distance parallel to runway centerline
x_c = distance at which a control motion is initiated
y = distance perpendicular to runway centerline
β = yaw angle of nose tire
δ_0 = vertical tire deflection for pure vertical loading conditions
δ_l,δ_r = vertical deflections for left and right tires
δ_a = average vertical deflection ($= (\delta_l + \delta_r)/2$)
μ = friction coefficient between a skid and the runway
Φ = angle between vehicle track and runway centerline
ψ = yaw angle of vehicle with respect to its track

Subscripts

m,n = main gear and nose gear, respectively
l,r = left tire and right tire, respectively
0 = initial conditions

Presented as Paper 69-790 at the AIAA Aircraft Design and Operations Meeting, Los Angeles, California, July 14–16, 1969; submitted August 1, 1969; revision received December 12, 1969.
* Aero-Space Technologist.

Introduction

A FAIRLY extensive effort has been made in recent years to develop landing devices for aerodynamic lifting vehicles that undergo severe aerodynamic heating, such as the X-15 and the X-20 (Dyna Soar). Since these two vehicles were intended to land horizontally on a lakebed, where the runout area is practically unlimited in both distance and direction, they were designed without steering capability. Operation on this type of landing area requires only that the vehicle be directionally stable, so that it will not yaw uncontrollably and roll over. The proposed lifting-body reentry orbiting vehicles, however (HL-10, M_2/F_2, SV-5, for examples), have landing footprint areas which could cover much of the United States, and it is being proposed that any long airport runway should be capable of serving as a landing site for such vehicles returning from orbit. To make such operations on runways feasible, the vehicle must be equipped with a landing gear that is directionally stable and steerable, so that the vehicle will not leave the runway because of initial misalignment, crosswind, runway crown, etc.

The advantages in weight and simplicity which led to the use of skids on the main gear of the X-15 and X-20 also make skids attractive for the newer lifting-body vehicles. There

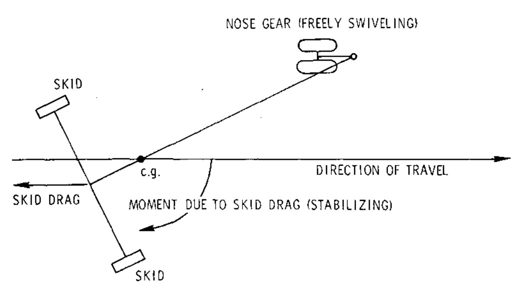

Fig. 1 Directional stability of an X-15-type landing gear.

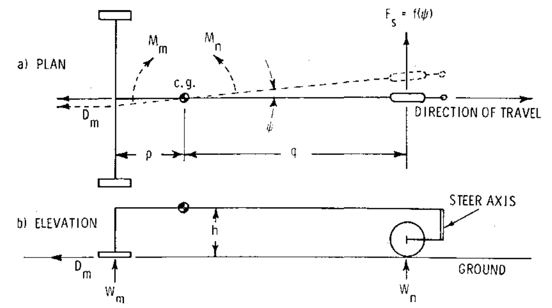

Fig. 2 Conventionally steered gear with main gear skids. Steering straight ahead.

has not been available, however, a landing gear with main gear skids which meets the twin requirements of directional stability and steerability. A method has been devised for providing a reentry vehicle with a landing gear that would use main gear skids and would provide steering during the landing runout. The method is described, and results from a preliminary computer study of the steering effectiveness of this method, if applied to the existing HL-10 vehicle, are given. Also described is a new type steerable nose gear for use in this system, and test results of a prototype of this gear are presented.

Considerations of Directional Stability

This section discusses the directional stability during slideout of *a*) one type of landing gear which has previously been used on vehicles with skids on the main gear and tires on a freely castoring nose gear, and *b*) the directional instability that is encountered when a vehicle with main gear skids is equipped with a conventionally steered nose gear with wheel and tire. The X-15 has the former type of landing gear. Figure 1 depicts the vehicle traveling in a yawed attitude. Since the nose gear is allowed to castor freely, no side force can be developed, and only a small rolling drag exists. The only force of consequence acting between the airplane and the ground is the drag of the main gear skids, which gives rise to a directionally stabilizing moment around the c.g. which tends to reduce yaw angle and realign the airplane with the direction of travel. Hence, the airplane is directionally stable, but does not have ground steering capability.

Figure 2 shows a landing gear with main gear skids and conventional nose gear steering. In a conventional airplane steering system, the angle of steer is hydraulically controlled to follow the pilot's steering input. From the standpoint of directional stability, therefore, the gear is always locked with respect to the vehicle at the steer angle corresponding to pilot control input, and cannot change heading in response to ground forces to provide any directional stability. Let us consider that the vehicle, which is here assumed to be steered straight ahead, is rotated to the position shown by the dashed lines in the plan view, but the direction of travel remains the same. If the gear is directionally stable, the vehicle will return to zero heading without any pilot steering input. If the gear is directionally unstable, the vehicle heading, ψ, will diverge, and the vehicle will go into a ground loop. With the vehicle rotated, the nose gear is still in the zero steer position, so the tire is now traveling at a yaw angle ψ and developing a side force F_s to produce a directionally destabilizing moment, M_n, around the c.g. The drag of the main gear skids, on the other hand, is developing a directionally stabilizing moment, M_m, around the c.g., and this moment must be equal to M_n for neutral directional stability and must be greater for positive stability.

Neglecting nose gear rolling resistance and assuming equal weight on each main gear skid for simplicity, the equation for the distribution of weight on the nose and main gears during slideout is

$$W_m p + D_m h = W_n q \tag{1}$$

from which

$$W_m/W_n = q/(p + \mu_m h) \tag{2}$$

As stated earlier, a necessary condition for the vehicle to have neutral directional stability is

$$M_m = M_n \tag{3}$$

therefore, from Fig. 2, the requirement for neutral stability is

$$D_m p \sin\psi_{\text{rad}} = F_s q = N\psi_{\text{rad}} q \tag{4}$$

where N is cornering power of the tire in lb/rad.

From data contained in Refs. 3–5, and using the definition of cornering force parameter, from Fig. 49 of Ref. 6, calculations of N were made for 34 combinations of Type VII tire size and ply rating. Tire size varied between 16 × 4.4 and 32 × 6.6, and vertical load rating varied between 1700 lb and 13,500 lb. All tires were considered to be operating at rated load, and a mean value of $N = 3.1W_n$ represents all the tires within ±12%. Using $N = 3.1W_n$ in Eq. (4)

$$\mu_m W_m p \sin\psi_{\text{rad}} = 3.1 W_n \psi_{\text{rad}} q \tag{5}$$

for small angles, $\sin\psi_{\text{rad}} = \psi_{\text{rad}}$ therefore Eq. (5) can be written as

$$W_m/W_n = 3.1q/\mu_m p \tag{6}$$

From Eqs. (2) and (6)

$$\mu_m = (1/3.1 - h/p)^{-1} \tag{7}$$

Solving Eq. (7) for various values of h/p yields the values of μ_m required for neutral stability; for example, $\mu_m = 3.1$, 4.5, and 13.7 for $h/p = 0$, 0.10, and 0.25, respectively. When $h/p = 0$, the c.g. lies in the ground plane, and there is no load transfer from the main gear to the nose gear. The very large value of skid friction coefficient required for this condition ($\mu_m = 3.1$) is unobtainable, and the required friction coefficient becomes larger as h/p increases. These calculations indicate that a vehicle equipped with main gear skids and a conventionally steered nose gear of the type considered in this section will be in unstable equilibrium at zero steer angle and zero vehicle yaw angle. Any disturbance would lead to diverging yaw angle and ground looping. The gear is therefore unsuitable for use. Model tests have demonstrated this effect.

Method of Steering Using Controlled Nose Gear Side Force

Because neither of the preceding two landing gears can be used to obtain both runout stability and steering, a new concept of a pilot-selected constant steering force at the nose

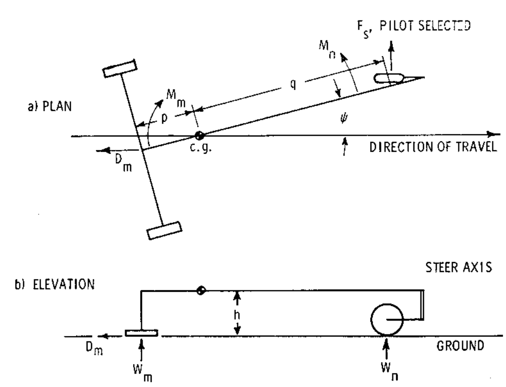

Fig. 3 A new concept for directionally stable steering.

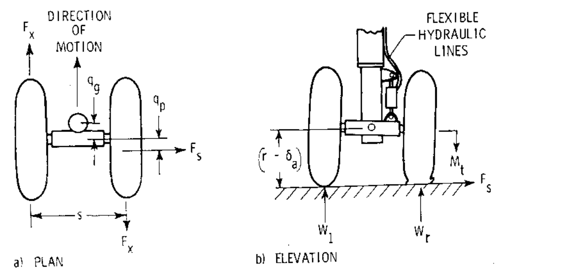

Fig. 4 Stable steering by differential deflection of corotating pneumatic tires.

gear (Fig. 3) is being investigated. (Means for obtaining a constant steering force at the nose gear are discussed in the next section.) The directional stability of this gear will be examined. From the elevation in Fig. 3, an equation for the weight on the main gear, W_m, during slideout may be written, as was done for Fig. 2. Cosine effects are considered negligible for the values of ψ to be encountered.

$$W_m p + D_m h = W_n q \tag{8}$$

Since $W_m + W_n = W$, Eq. (8) reduces to

$$W_m = Wq/(p + q + \mu_m h) \tag{9}$$

The condition for directional balance of moment, that is, $M_m = M_n$, may be written as follows:

$$D_m p \sin\psi = F_s q \cos\psi \tag{10}$$

Substitution from Eq. (9) yields

$$\tan\psi = F_s q/\mu_m W_m p = F_s(p + q + \mu_m h)/\mu_m p W \tag{11}$$

Equation (11) indicates that, under the influence of ground forces alone, ψ during slideout would be a constant for a selected value of F_s, since all other quantities in Eq. (11) are constant.

From the foregoing discussion, it can be concluded that the concept of pilot-selected constant F_s will make it possible to provide directionally stable steering during landing runout of any vehicle which is aerodynamically stable. Steering is accomplished by this F_s and by the aerodynamic side force which is developed as a result of the yaw angle ψ induced by F_s.

Differential Deflection of Corotating Pneumatic Tires on Nose Gear

This type of steering offers a simple way to develop a controlled side force at the nose gear. The fact that the rolling radius of a pneumatic tire decreases as the vertical deflection is increased makes it possible to steer a corotating wheel gear by differentially loading the two tires as shown schematically in the elevation view of Fig. 4. Under these conditions, the gear will roll in a circle to the right, as viewed in the plan of

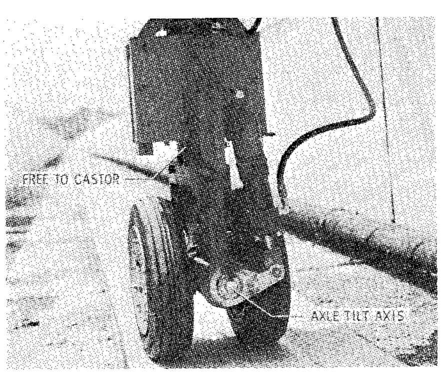

Fig. 5 Prototype gear installed for research runs.

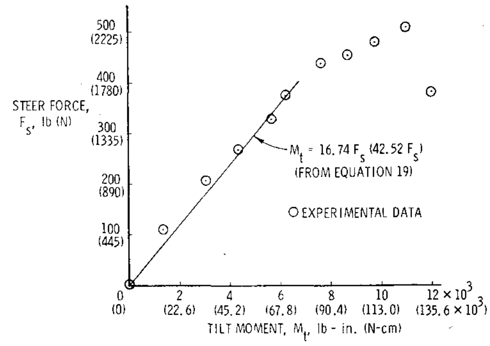

Fig. 6 Variation of steer force, F_s, with applied axle tilt moment, M_t, for prototype gear. F_z = 2000 lb (8900 N); tire pressure = 90 psi (62 N/cm²); test speed = 22 knots.

Fig. 4, or if forced to follow a straight line, will develop an F_s to the right as shown. A simplified analysis may be made to show the general nature of the relationship between the moment M_s applied to tilt the axle and the F_s developed. (A patent application on this type of nose gear has been filed.)

The rolling radius of a tire which is developing a drag or braking force is given in Ref. 6, Eq. (76a) as follows:

$$r_e = r - (\delta_0/3) + F_x/K_x \tag{12}$$

Similarly, for a tire developing a thrust or driving force, the rolling radius would be

$$r_e = r - (\delta_0/3) - F_x/K_x \tag{13}$$

For the case where the gear is traveling in a straight line, the two tires must assume the same rolling radii, since they are turning at the same rpm. Hence, from Eqs. (12) and (13) and with proper substitutions for the deflection,

$$2(F_x/K_x) = (\delta_r - \delta_l)/3 \tag{14}$$

Again, from Ref. 6, Figs. 10–14, as a first approximation, the deflection of a tire may be assumed to be proportional to the load in the region of rated deflection, or $\delta_0 = C_1 W$. Substituting this approximation in Eq. 14,

$$W_r - W_l = 6F_x/C_1 K_x \tag{15}$$

Referring now to the plan of the gear in Fig. 4a, an equation may be written for a balance of moments around the castor axis at the center of the landing gear strut:

$$F_{xs} = F_s(q_g + q_p) \tag{16}$$

where q_g and q_p are the geometric castor and pneumatic castor, respectively. Substituting Eq. (16) in Eq. (15)

$$W_r - W_l = 6F_s(q_g + q_p)/C_1 K_x s \tag{17}$$

Now referring to the elevation of the gear in Fig. 4b, an equation may be written for the balance of moments around

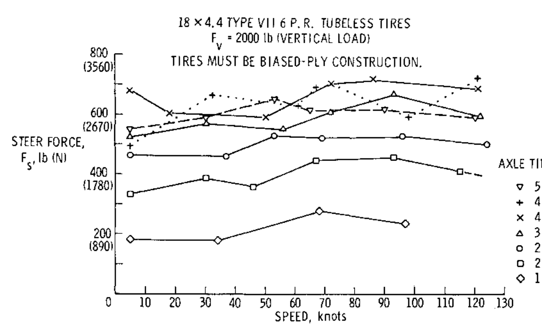

Fig. 7 Steer force developed by corotating wheel tilt-axle nose gear.

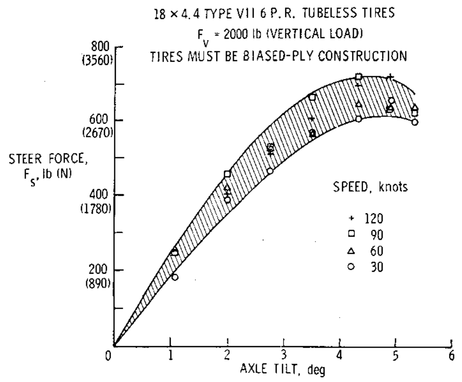

Fig. 8 Steer force developed by corotating wheel tilt-axle nose gear.

the tilt axis of the axle as follows

$$W_r s/2 + F_x(r - \delta_0) = W_l s/2 + M_t, \text{ or}$$
$$W_r - W_l = 2/s[M_t - F_s(r - \delta_0)] \qquad (18)$$

Equating Eqs. (17) and (18), we get

$$M_t = F_s[3(q_g + q_p)/C_1K_x + (r - \delta_0)] \qquad (19)$$

Thus, the F_s developed will be a linear function of the applied axle tilt moment M_t. Some variations from linearity are expected, because of the simplifying assumptions, and there may be a velocity effect.

A prototype gear (Fig. 5) using HL-10 hardware (tires, wheels, axle) has been built and tested at speeds up to 125 knots. The data for $F_s(M_t)$ in Fig. 6 were obtained from a preliminary investigation at low speed with the prototype gear mounted on a truck. A given M_t was applied, and the axle was free to tilt. The experimental data agree quite well with the analytical curve calculated from Eq. (19). The gear showed a tendency toward shimmy with this method of operation, so in a later investigation at the Langley landing loads track at speeds up to 125 knots, the axle was tilted a fixed amount, and the side force developed was measured. The gear was free from shimmy with this mode of operation. The results from the landing loads track investigation, giving steer force as a function of speed for various axle tilts, are presented in Fig. 7. The data points are connected by straight lines for ease in identification, with no attempt at fairing. The data of Fig. 7 are cross-plotted against axle tilt in Fig. 8. The plotted points in Fig. 8 represent the intersections of the lines with the designated speed on Fig. 7; they do not represent data points, except coincidentally in a few instances. From Fig. 8, it would seem that axle tilt should be limited to about 3.5°; at this tilt angle, most of the maximum available steer force is obtainable, and both tires are still firmly on the ground to prevent shimmy. The results presented in Figs. 6–8 show that a maximum F_s of about 500 lb was obtained for the test conditions, which should be adequate for HL-10 usage.

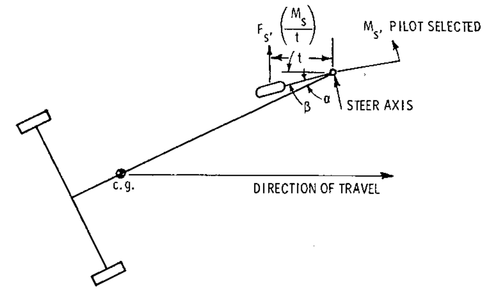

Fig. 9 Stable steering achieved by controlling steering moment.

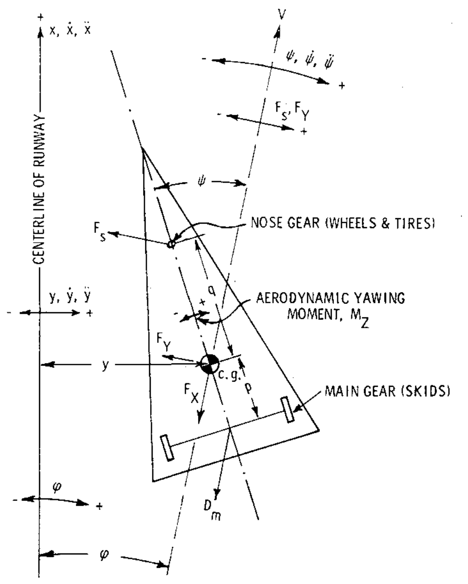

Fig. 10 Vehicle and runway descriptive quantities used in analog study.

The nose gear is at all times free to castor with respect to the vehicle, and develops steering force solely as a result of ground forces and of the applied M_t. It therefore meets the requirements for controlled-force steering as described earlier.

Pilot Selection of Steering Torque

If the steering control is arranged so that the pilot selects the steering moment M_s applied about the steer axis, rather than by selecting nose wheel steering deflection with respect to the vehicle, as in conventional steering, then by reference to Fig. 9 it can be seen that

$$M_s = F_s t \qquad (20)$$

Thus, the F_s developed by the nose wheel is proportional to the pilot-selected M_s. The steering mechanism would compensate for any perturbations in yaw angle ψ and maintain M_s at the pilot-selected value. Since $F_s \propto M_s$, F_s is effectively under control of the pilot and is independent of ψ. If the nose wheel is equipped with a pneumatic tire, the ability of the tire to develop an F_s when traveling at an angle, β, as in Fig. 9, will be immediately recognized. This is well documented.

If, on the other hand, it is desired to use a wire brush wheel on the nose gear, the ability of this wheel to develop a side force is not well documented. However, consideration of the manner in which the wires are deformed laterally during passage through the footprint of a wheel which is rolling in a yawed attitude indicates that a side force will definitely be developed. The amount of side force that can be developed by a wire brush wheel would need to be determined from experiment.

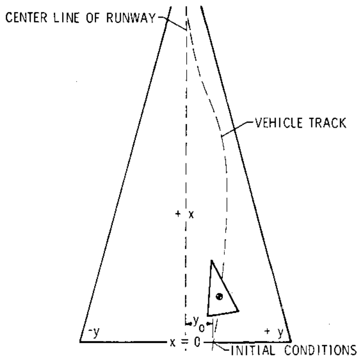

Fig. 11 Vehicle run-out on runway as in analog study.

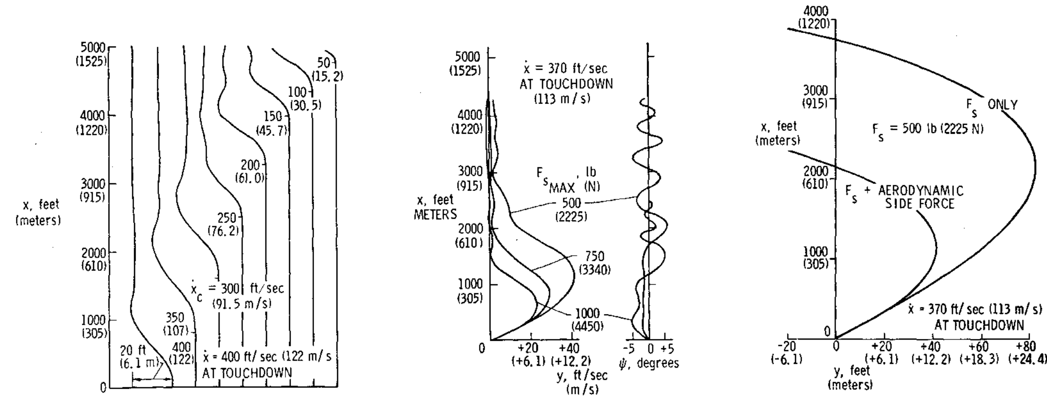

Fig. 12 Results from analog study. $u = 0.4$, $q/(q + p) = 0.7$. $F_{s\max} = 500$ lb (2225 N).

a) 20 ft (6.1 m) offset maneuver at different values of $\dot{x}_c$.

b) Steering to correct a drift of $\dot{y} = +25$ fps (+ 7.6 m/sec).

c) Effectiveness of aerodynamic side force in steering. initial drift of $\dot{y} = +25$ fps (7.6 m/sec).

Analog Computer Studies of Constant Force Steering Concept

A mathematical model (Fig. 10) of the HL-10 flight vehicle was programed on an analog computer. The runout of the vehicle is shown schematically in Fig. 11. The various forces, moments, and dimensions indicated in Fig. 10 were incorporated in the following three equations to form a basis for the analog computer to generate time histories of the airplane velocity and position, both parallel and perpendicular to the centerline of the runway, and of yaw angle:

$$\ddot{x} = g/w[-D_m \cos\Phi - F_s \sin\Phi - F_D \cos\Phi - F_Y \sin\Phi]$$

$$\ddot{y} = g/w[-D_m \sin\Phi + F_s \cos\Phi - F_D \sin\Phi + F_Y \cos\Phi]$$

$$\ddot{\psi} = 1/I[-D_p \sin(\psi - \dot{\psi}p \cos\psi/V) + F_s q \cos\psi + M_z + M\dot{\psi}]$$

Figures 12a–12c show sample results for the vehicle track during landing runout; x is the distance from the point of touchdown, and y is the distance of the vehicle from the runway centerline. The results shown in Fig. 12a represent a simple offset maneuver, where the pilot desires to displace his track 20 ft laterally in order to put the vehicle on the runway centerline. The velocity at touchdown ($x = 0$) is 400 fps in all eight cases, but the steering maneuver is initiated at a variety of speeds, $\dot{x}_c$, as indicated. It is seen that the desired offset is accomplished at all speeds with a steering force, $F_{s_{\max}}$, of 500 lb, which was shown (Figs. 6–8) to be within the capability of a nose gear of this configuration.

A maneuver to correct side drift at touchdown is shown by the results in Fig. 12b. The vehicle touches down with a lateral velocity, $\dot{y}$, of +25 fps and, for each curve, the pilot immediately applies the maximum F_s, as indicated on the curve. The steering force subsequently was modulated by the pilot while watching the vehicle track on the computer, and the tracks shown were generated. The right side of the figure shows $\psi(x)$; the maximum ψ encountered is $\pm 6°$.

It was realized that F_s produced only a part of the total lateral force on the vehicle, and that an aerodynamic lateral force was being developed. To assess the relative importance of these forces in steering the vehicle, some runs were made with the aerodynamic side force disconnected in the computer, so that F_s was the only lateral force acting on the vehicle. A sample of these results is shown in Fig. 12c. In these runs, the initial $\dot{y}$ was +25 fps, and F_s was held constant throughout the runout. With F_s acting alone, the lateral drift was 95% greater, and the distance along the runway when the vehicle was brought back to the center line was 78% greater, than when aerodynamic side force also was acting. Thus, F_s acts in conjunction with the induced aerodynamic force to accomplish steering at high speed and, as shown in Fig. 12a, the gear alone can steer at the lower speeds where aerodynamic forces are not available.

These few samples of results from the analog study of the steerable main skid gear applied to the HL-10 vehicle show that 1) steering can be accomplished at all speeds, and 2) the vehicle is directionally stable and operates with yaw angles no larger than about 6°.

The work in Ref. 8, which was based on the work in Refs. 1 and 7, examined the influence of a number of airplane parameters on the performance of a controlled force steering system.

Conclusions

The new concept of steering by selecting and maintaining a nose gear lateral steering force, rather than by selecting a nose gear steer angle, has been shown by tests and by analysis to be applicable to the problem of steering a vehicle with skids on aft-mounted main gears. Such a vehicle can be steered in a stable manner by the new system, whereas the conventional method of steering renders the vehicle directionally unstable.

A method has been devised for developing a selected steering force by differential vertical deflection of corotating tires on the nose gear. Simplified analysis of the steering action of the gear, tests of a prototype gear at speeds up to 125 knots, and analog studies of the steering of the HL-10 vehicle all show that this nose gear can be successfully applied to steer a vehicle with main gear skids, making runway landings feasible.

References

[1] Joyner, U. T., Nose Gear Steering System for Vehicle With Main Skids, Sept. 28, 1965, U.S. Patent No. 3,208,694.

[2] Dreher, R. C. and Batterson, Sidney A., "Coefficients of Friction and Wear Characteristics for Skids Made of Various Metals on Concrete, Asphalt, and Lakebed Surfaces," TN D-999, 1962, NASA.

[3] *1965–66 Year Book*, The Tire and Rim Association, Akron, Ohio.

[4] *Aircraft Tire Handbook, 1963*, The Goodyear Tire and Rubber Co., Akron, Ohio.

[5] *Aircraft Tires Engineering Data*, 2nd ed., B. F. Goodrich, Akron, Ohio.

[6] Smiley, R. F. and Horne, W. B., "Mechanical Properties of Pneumatic Tires With Special Reference to Modern Aircraft Tires," TR R-64, 1960, NASA.

[7] Stubbs, S. M., "Landing Characteristics of a Dynamic Model of the HL-10 Manned Lifting Entry Vehicle," TN D-3570, 1966, NASA.

[8] Feld, D. J., "Steering Control of Skid-Equipped Horizontally Landing Spacecraft," *Journal of Spacecraft and Rockets*, Vol. 5, No. 9, Sept. 1968, pp. 1103–1106.